J Atmos Chem (2009) 64:107–127
DOI 10.1007/s10874-010-9172-z

Continuous observations of water-soluble ions in $PM_{2.5}$ at Mount Tai (1534 m a.s.l.) in central-eastern China

Yang Zhou · Tao Wang · Xiaomei Gao · Likun Xue · Xinfeng Wang · Zhe Wang · Jian Gao · Qingzhu Zhang · Wenxing Wang

Received: 7 June 2010 / Accepted: 22 September 2010 /
Published online: 8 October 2010

Abstract Near real-time measurements of $PM_{2.5}$ ionic compositions were performed at the summit of the highest mountain in the central-eastern plains in the spring and summer of 2007 in order to characterize aerosol composition and its interaction with clouds. The average concentrations of total water soluble ions were 27.5 and 36.7 $\mu g m^{-3}$, accounting for 44% and 62% of the $PM_{2.5}$ mass concentration in the spring and summer, respectively. A diurnal pattern of SO_4^{2-}, NH_4^+ and NO_3^- was observed in both campaigns and attributed to the upslope/downslope transport of air mass and the development of the planetary boundary layer (PBL). The average SO_2 oxidation ratio (SOR) in summer was 57% (±27%), more than twice that in spring 24% (±16%); the fine nitrate oxidation ratio (NOR) was comparable in the two seasons (9±6% and 11±10% in summer and spring, respectively). This result indicates strong summertime production of sulfate aerosol. A principal component analysis shows that short-range and long-range transport of pollution, cloud processing, and crustal source were the main factors affecting the variability of the measured ions (and other trace gases and aerosols) at Mt. Tai. Strong indications of biomass burning were observed in summer. Cloud scavenging rates showed larger variations for different ions and in different cloud events. The elevated concentrations of the water soluble ions at Mt. Tai indicate serious aerosol pollution over the North China plain of eastern China.

Keywords Real-time measurements · Cloud scavenging · Mt. Tai · Fine aerosol · North China Plain · Biomass burning

Y. Zhou · T. Wang (✉) · X. Gao · L. Xue · X. Wang · Z. Wang · Q. Zhang · W. Wang
Environment Research Institute, Shandong University, Ji'nan, Shandong 250100, China
e-mail: cetwang@polyu.edu.hk

T. Wang · X. Gao · L. Xue · X. Wang
Department of Civil and Structural Engineering, The Hong Kong Polytechnic University, Hong Kong, China

T. Wang · J. Gao · W. Wang
Chinese Research Academy of Environmental Sciences, Beijing 100012, China

1 Introduction

Aerosols influence global climate directly by scattering and absorbing solar radiation and indirectly by modifying the properties of cloud condensation nuclei (CCN) (Andreae and Rosenfeld 2008); they also reduce visibility and adversely affect human health. Fine particles ($PM_{2.5}$, particulate matter with an aerodynamic diameter smaller than or equal to 2.5 μm) are of particular concern due to their ability to penetrate deeper into the respiratory tract and because of their larger contribution to visibility reduction, compared to larger size particles (Watson 2002; Nel 2005). In urban areas, about half of the $PM_{2.5}$ mass consists of water-soluble ions (Zhang et al. 2007). These water-soluble species affect the hydroscopic nature and acidity of aerosols which in turn determine their lifetime and their chemical and optical properties (Ocskay et al. 2006). Major water-soluble species in fine particles such as sulfate, ammonium, and nitrate are secondary pollutants resulting from reactions involving primary precursors, namely, sulfur dioxide (SO_2), nitrogen oxides (NO_x), and ammonia (NH_3).

With the rapid economic growth, the emissions of SO_2 and NO_x in China have increased from 2001 to 2006 by 36% and 55%, respectively (Zhang et al. 2009). In 2006, anthropogenic emissions from China contributed 66% and 57% for SO_2 and NO_x to Asian emissions (Zhang et al. 2009), and 49% for NH_3 in 2000 (Streets et al. 2003). The strongest emissions are in the central-eastern plains which contain three megacities (Beijing, Tianjin, and Shanghai), and parts or the entirety of the provinces of Hebei, Shandong, Henan, Hubei, and Jiangsu (Fig. 1). Mount Tai (36° 16′ N, 117° 6′ E, 1534 m a.s.l.), is the highest mountain on the central-eastern plains (Fig. 1). It is an ideal location to study regional-scale atmospheric processes affecting the transport and fate of air pollution and the study of aerosol-cloud interactions. Previous studies have revealed serious pollution at Mt. Tai in terms of photochemical ozone (Gao et al. 2005; Li et al. 2007), particulate matter (Xu et al. 2008), and acidic rain (Wang et al. 2008).

In measuring the ambient concentrations of aerosols, conventional filter-based methods require sampling over long periods of time, and have several shortcomings. Filter-based methods have increased sampling artifacts, including negative artifacts due to losses of semi-volatile components from the filter medium and positive artifacts due to absorption and/or conversion of gases on the filter. These methods also have a lower time resolution, which makes it difficult to study correlation between particle

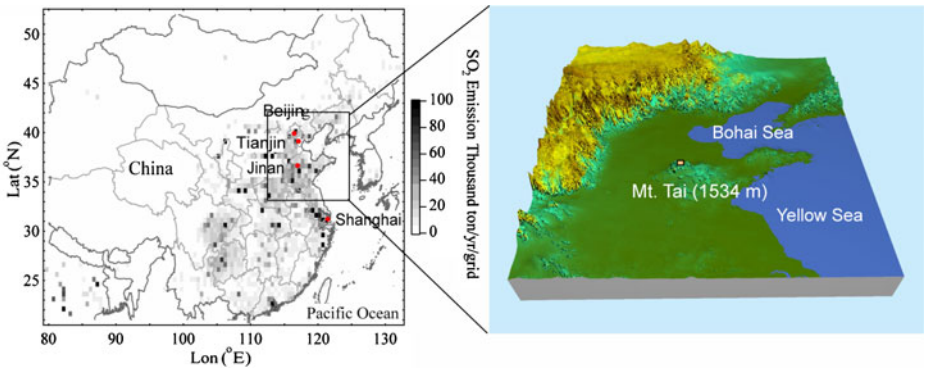

Fig. 1 Location of the observation site at the summit of Mount Tai in central-eastern China and Asian SO_2 emission intensity in 2006 (Zhang et al. 2009)

composition and changes in emissions, and chemical and transport processes that can occur over short-time scales (Lee et al. 2008). To overcome these drawbacks, a variety of semi-continuous instruments have been developed and applied for field measurements of aerosol ionic composition (Weber et al. 2001; Orsini et al. 2003; Solomon and Sioutas 2008).

As part of China's National Basic Research Program (the 973 Program) on acid rain pollution and control, we carried out the real-time measurements of the water-soluble inorganic compounds at the top of Mt. Tai in conjunction with measurements of trace gases, continuous $PM_{2.5}$, organic carbon (OC) and elemental carbon (EC), and meteorological parameters. In this study, we analyze the continuously measured data on $PM_{2.5}$ water soluble ions, and compare the results of real-time instrument and a filter-based sampling method. Continuous data was also used to show diurnal variations in spring and summer, and principal component analysis (PCA) is used to examine the major sources or processes that affected the variability of the gases and aerosol. We estimate the scavenging rates of major inorganic ions and organic aerosol by clouds/fogs, and examine the impact of biomass burning at this high-elevation site.

2 Methodology

2.1 Measurement site

Mt. Tai (1534 m a.s.l.) is located 15 km north of the city of Tai'an (population ~ 500,000), and is 230 km away from the Bohai and Yellow Seas (Fig. 1). The measurement site was situated in an infrequently visited meteorological observatory at the summit of the mountain, and away from most local pollution sources (Ren et al. 2009). Experiments were conducted from March 21 to April 23 (spring campaign) and from June 15 to July 15 (summer campaign) in 2007.

2.2 Real-time ion measurements

$PM_{2.5}$ ionic composition was measured on an hourly basis using an ambient ion monitor (AIM; Model URG 9000B, URG Corporation), which is similar to the one used by Wu and Wang (2007). The ambient air samples were drawn at a height of 4 m above the ground through a cyclone (cut size: 2.5 μm) at a flow rate of 3 $L min^{-1}$. To minimize the loss of particles during sampling, a Teflon coated aluminum pipe (length: 2 m, inner diameter: 2 cm) was used for sampling and was set up in the vertical direction. The particles first entered a denuder, which removes acidic and alkaline interfering gases prior to collection of particles. The air flow was then mixed with supersaturated steam to form water droplets. The droplets were subsequently collected into two syringes every hour by a cyclone condenser. The particles dissolved into 8.7 mL liquid and the solution was collected by the two syringes every hour. The solutions were injected into two ion chromatographs (Dionex, IC90) to detect the major inorganic ions present, including F^-, Cl^-, NO_2^-, NO_3^-, SO_4^{2-}, Na^+, NH_4^+, K^+, Mg^{2+} and Ca^{2+}. Anions were analyzed by an Ionpac AG/AS14A column, an AMMS 300 4-mm suppressor, and a conductivity detector with an eluent of 3.5 $mmol L^{-1}$ Na_2CO_3/1.0 $mmol L^{-1}$ $NaHCO_3$ (Merck KGaA, Darmstadt, Germany) at a flow rate of 1.2 $mL min^{-1}$. Cations were measured by an IonPac CG/CS12A column, a CSRS Ultra II-4 mm suppressor, and a conductivity detector with an eluent of 20 $mmol L^{-1}$ methanesulfonic acid (Fluka Co.) at a flow rate of 1.0 $mL min^{-1}$.

The minimum detection limit (MDL at the 99% confidence limit) of this method was determined by sampling zero air (TEI, Model 111). Standard deviations (s) for each ion were obtained, and 3 s was considered as the MDL for that ion. The MDL for SO_4^{2-}, NO_3^- and NH_4^+ is 0.054, 0.010 and 0.045 $\mu g m^{-3}$ respectively. MDL ranged from 0.002 to 0.338 $\mu g m^{-3}$ for other ions (Cl^-, Na^+, K^+, Mg^{2+} and Ca^{2+}). Multi-point calibrations were carried out every 4 days after the eluent solutions were changed. The measurement uncertainty of the AIM was estimated to be approximately ±10% according to the method described in Trebs et al. (2004), which included the uncertainties in the determinations of the concentration of solution by the IC, the volume of solution, and the air flow rate. However, the uncertainty for sulfate in the spring season may be larger than above value due to the positive interference by the high SO_2 concentrations in spring at Mt. Tai, as to be shown later.

The AIM collected data every hour from March 22 to April 23 and from June 16 to July 15, except during April 9–15 due to an AIM failure. A total of 618 and 702 hourly samples were collected in the spring (25 days) and summer (30 days), respectively.

2.3 Filter-based ion measurements

For comparison to real-time measurements, $PM_{2.5}$ samples were collected on Teflon membranes using a commercially available filter-based sampler (Reference Ambient Air Sampler, Model RAAS 2.5–400, Thermo Andersen). This sampler has been used by our group in China (Wu and Wang 2007; Nie et al. 2010) and by other researchers in the US (e.g., Anderson et al. 2002). The sampler does not have a denuder to remove gases prior to sampling filter or a backup filter to collect vapor from the sampled aerosol, thus can subject to both positive and negative artifacts. The magnitude of these artifacts depends on the chemical characteristics (mass and composition) of aerosols and meteorological conditions (Tsai and Perng 1998; Pathak and Chan 2005; Nie et al. 2010). In general, the sampling artifact for sulfate is negligible. For nitrate and other semi-volatile species, absorption of vapor such as HNO_3 can cause positive artifact, and on the other hand, evaporation of NH_4NO_3 leads to negative bias which can be substantial (45–75%) at high temperature and at low aerosol loading (Saarnio et al. 2010; Nie et al. 2010). The measurements uncertainties for the most of the ions are ±10% (Vecchi et al. 2008), but could be larger for nitrate and ammonium. As to be shown in Section 3.1.1 by a comparison with the AIM data, sampling artifacts for ammonium nitrate in the RAAS were generally less than 20% for most of the samples, in part because of relatively low temperatures at the top of Mt. Tai.

The sampling time was about 24 h, normally from 9:00 a.m. to 8:45 a.m. of the next day. Several shorter-time sampling runs were also conducted. The samples were put in polyethylene boxes immediately after sampling and stored at −5°C. The Teflon filters were weighed with an electronic microbalance (Sartorius-ME5, ± 1 μg) after equilibrating the filter at constant temperature (20±0.5°C) and humidity (50±2%) for over 24 h. A total of 61 filter samples were collected during the two campaigns.

The Teflon filters were extracted ultrasonically in 20 mL deionized water (resistivity >18 MΩcm). The solution was filtered through a microporous membrane (pore size, 0.2 μm) into a clean polycarbonate bottle. All samples were stored at 4°C before chemical analysis. The same chromatographs used above were used for analysis of the major inorganic ions; the MDL ranged from 0.004 to 0.01 $\mu g m^{-3}$ for the filter samples. The measurements uncertainties are estimated to be ±10% for most of the ions (Vecchi et al. 2008), but nitrate may have a larger uncertainty.

2.4 Measurements of other atmospheric and meteorological parameters

The instruments for measuring ozone (O_3) (TEI, Model 49C), carbon monoxide (CO) (API Model 300E), and sulfur dioxide (SO_2) (TEI, Model 43C) have been described previously (Wang et al. 2003a; Gao et al. 2005). Total reactive nitrogen (NO_y) was measured with a chemiluminescence analyzer equipped with an externally placed molybdenum oxide (MoO) catalytic converter (TEI, Model 42Cy). OC and EC aerosols were analyzed by a Semi-Continuous OC/EC Analyzer (Sunset-DOSCOCEC, Sunset Lab, Portland, OR) (Wang et al. manuscript in preparation). In the present study we used the data on non-volatile organic carbon. Total peroxides were measured with a fluorometric analyzer based on para-hydroxyphenylacetic acid (POPHA) and horseradish peroxidase derivatization and fluorescence detection (Lazrus et al. 1986; Ren et al. 2009). The mass concentrations of $PM_{2.5}$ were continuously measured by a TEOM 1400a ambient particulate monitor (Rupprecht & Patashnick Co., Inc., Albany, NY). This instrument contained a device which has been shown to be able to recover and include semi-volatile compounds in the measurement of $PM_{2.5}$ mass (Wilson et al. 2006; Grover et al. 2006). Meteorological measurements were obtained by the staff at the Mt. Tai Meteorological Observatory.

3 Results and discussion

3.1 General results

3.1.1 Comparison of real-time and filter-based measurements

Hourly data from the AIM were averaged over the period matching the collection time of filter samples (usually 24 h). Figures 2, 3 and 4 show scatter plots comparing the two methods for sulfate, nitrate, and ammonium concentrations in the spring and summer campaigns. Good to strong correlations were found between the two methods with correlation coefficients (R^2) ranging from 0.52 to 0.99; the slopes of the comparative data, which were determined using the reduced matrix axis method (Hirsch and Gilroy 1984), ranged from 0.76 to 1.64.

Wu and Wang (2007) reported that the AIM exhibited positive interference at high concentrations of SO_2 (i.e., >30 ppbv) and negative readings at high loadings of particulate matter (e.g., sulfate >20 $\mu g\,m^{-3}$). In the present study, the SO_2 interference problem was present in the spring campaign because elevated SO_2 concentrations were frequently observed at Mt. Tai. As shown in Fig. 2a, spring AIM sulfate concentrations were substantially larger than those from the filter-based data (slope=1.64). The average SO_2 concentration in spring was 15 ppbv, with 67% of the values greater than 10 ppbv. Tests on site showed that SO_2 concentrations higher than 10 ppbv caused a positive bias in the sulfate measurements. As shown in Fig. 2b, the data with large AIM to filter ratios correspond to elevated SO_2 concentrations. In comparison, SO_2 concentrations during summer were lower (mean=8 ppbv), and no interference was observed, with a slope near unity. We have corrected the springtime hourly AIM sulfate data by dividing the AIM data by time-interpolated AIM to filter ratios. The analysis in the following sections is based on the corrected sulfate dataset.

Nitrate concentrations from the AIM and filter-based method showed strong correlations (R^2=0.92) in both campaigns and exhibited the same RMA slope; these data are plotted together in Fig. 3. The slope was 0.76 indicating that the AIM nitrate concentrations were

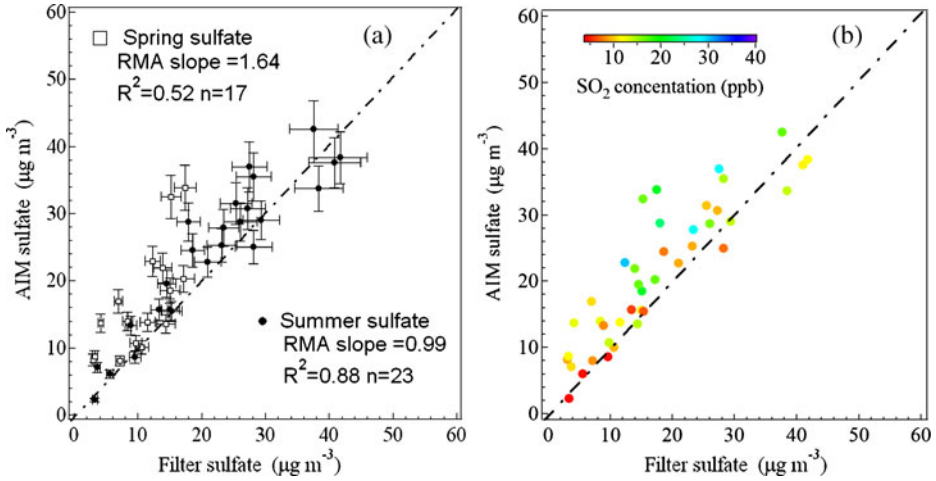

Fig. 2 Scatter plots of sulfate (SO_4^{2-}) from real-time and filter-based measurements: **a** spring and summer; **b** color-coded according to SO_2 concentration. *Error bars* stand for 10% uncertainty for AIM and RAAS

lower than those from the filter samples. The higher nitrate concentrations on filter may be due to the absorption of nitric acid on the filter and/or its reaction with particles. On the other hand, for a few samples with relatively low mass concentrations and collected at high temperature and low humidity (see color code in Fig. 3), the AIM nitrate was higher than the filter result, which can be explained by the commonly observed evaporative loss of nitrate from the filters.

Ammonium data from the AIM and the filter-based method compared well in both spring and summer (R^2=0.95), except for three samples collected during a dust storm in spring, where the AIM indicated higher values (see Fig. 4). It is worth noting that for those samples which showed higher nitrate values from the AIM, ammonium agreed well from

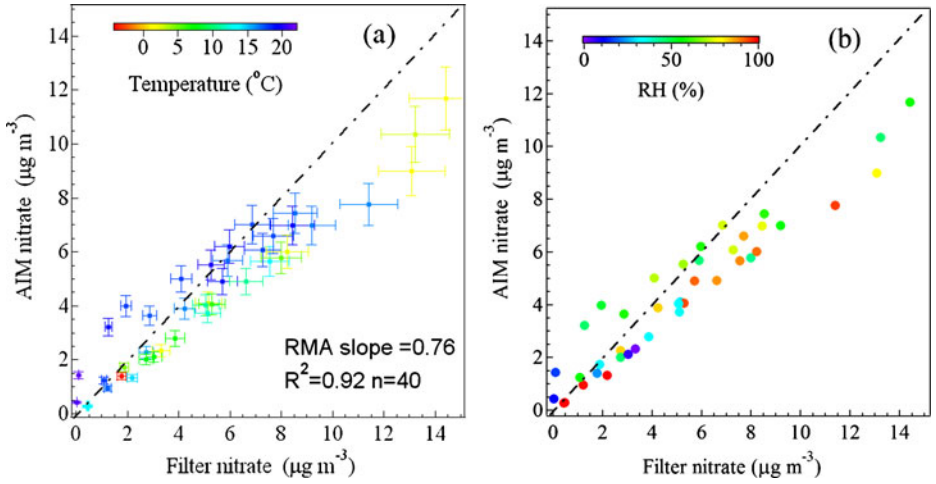

Fig. 3 Scatter plots of nitrate (NO_3^-) from real-time and filter-based measurements in spring and summer: **a** color coded by temperature; **b** color coded by relative humidity. *Error bars* stand for 10% uncertainty for AIM and RAAS

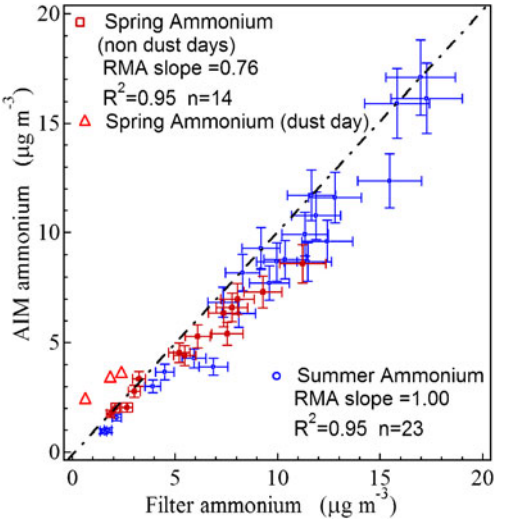

Fig. 4 Scatter plots of ammonium (NH_4^+) from real-time and filter-based measurements. *Error bars* stand for 10% uncertainty for AIM and RAAS

the two methods. This can be explained as follows. For these samples, the equivalence ratio of sulfate to nitrate were very high (8–14), indicating that most of NH_4^+ was in the form as $(NH_4)_2SO_4$. Thus some loss from the evaporation of ammonium nitrate would be evident in the comparison of the nitrate data, but negligible for ammonium.

For other ions, such as K^+, Ca^{2+}, and Mg^{2+}, the real-time and filter methods compared well (data not shown). Overall the RAAS sampler, which had no denuder and back-up filter, compared well with the AIM for ammonium and nitrate for most of the time during the study at Mt. Tai.

3.1.2 Concentrations of ionic species

Table 1 provides a statistical summary of the water-soluble ions measured during this study. In spring and summer, the mean $PM_{2.5}$ mass concentrations obtained from TEOM at Mt. Tai were 63.0 $\mu g m^{-3}$ and 59.3 $\mu g m^{-3}$, respectively; both are significantly higher than the newest US-EPA 24-h ambient air quality standard (35 $\mu g m^{-3}$). Water-soluble ions contributed a total of 44% and 62% to the $PM_{2.5}$ mass in spring and summer, respectively. Sulfate, nitrate, and ammonium contributed more than 90% of the total water-soluble ions measured. The mean K^+ concentrations were low in spring and summer (0.97 and 0.72 $\mu g m^{-3}$, respectively). The levels of Ca^{2+} and Mg^{2+} were close to their detection limits except during dust storm days, and sodium and chloride were also very low in spring and sometimes below the instrumental detection limit in summer (data not shown in Table 1).

Comparing the two seasons, the average concentration of water-soluble ions in spring is about 25% lower than summer. Significantly higher sulfate and ammonium concentrations were observed in summer compared to spring, while lower levels of nitrate were found in summer. Discussions on the formation of the fine sulfate and nitrate in the two seasons will be given in Section 3.2.

Table 2 compares the results from this study to those from other mountainous and ground-level sites. The ion concentrations measured at Mt. Tai rank highest compared with high-elevation rural sites in the USA (Lee et al. 2008), Japan (Tsuboi et al. 1996; Kido et al. 2001), or Finland (Teinila et al. 2004), and are significantly higher than the values reported

Table 1 Statistical summary of major ion concentrations in $PM_{2.5}$ ($\mu g m^{-3}$) at the summit of Mt. Tai in the spring and summer campaigns in 2007

Season[a]	Mean	Min	Max	Median	SD	Mean	Min	Max	Median	SD
			SO_4^{2-}					NO_3^-		
Spring[a]	12.76	[b]	51.21	11.74	8.83	5.81	0.02	28.13	4.72	4.71
Summer	22.92	0.01	74.67	19.02	16.73	4.03	[b]	20.70	2.98	4.00
			NH_4^+					K^+		
Spring	5.55	[b]	32.70	5.54	3.86	0.97	[b]	8.73	0.75	0.88
Summer	8.03	[b]	31.35	7.06	6.29	0.72	[b]	7.37	0.48	0.72
			Ca^{2+}					Mg^{2+}		
Spring	0.76	[b]	10.91	0.32	1.33	0.10	[b]	1.56	0.05	0.13
Summer	0.21	[b]	3.17	0.13	0.33	0.08	[b]	0.48	0.07	0.03

[a] Spring AIM data does not include April 10–15, 2007

[b] Below Minimum Detection Limit (MDL)

at two remote mountain sites in western China (Yang et al. 1996; Qu et al. 2009). The levels of the $PM_{2.5}$ ions at Mt. Tai are comparable to values in or near two mega-cities, Shanghai and Beijing (Wang et al. 2005; Wang et al. 2006; Pathak et al. 2009), but lower than concentrations measured in the city of Ji'nan (Yang et al. 2007), the capital of Shandong Province (60 km north of Mount Tai).

3.2 Formation mechanisms of sulfate and nitrate

To investigate factors controlling ionic formation, the diurnal variations of major ions, several trace gases, meteorological parameters, as well as the fine sulfate and nitrate oxidation ratios (SOR and NOR) were examined and are shown in Fig. 5. SOR and NOR are defined as the molar ratio of SO_4^{2-} and NO_3^- in $PM_{2.5}$ to the total oxidized sulfur and nitrogen, respectively, as

$$\mathrm{SOR} = [\mathrm{nss} - \mathrm{SO_4^{2-}}]/([\mathrm{nss} - \mathrm{SO_4^{2-}}] + [\mathrm{SO_2}]) \quad (1)$$

$$\mathrm{NOR} = [\mathrm{NO_{3_s}^-}]/[\mathrm{NO_y}] \quad (2)$$

where [nss-SO_4^{2-}] stands for the concentration of non sea-salt SO_4^{2-} in $PM_{2.5}$; and [NO_y] is the concentration of total reactive nitrogen, including NO, NO_2, PAN, HNO_3 and particulate NO_3^- and other forms of oxidized nitrogen (Wang et al. 2003b). A larger value of SOR and NOR indicates a larger conversion of SO_2 and NO_x to their respective particulate forms in $PM_{2.5}$.

SO_4^{2-}, NH_4^+ and NO_3^- (and other gases, Fig. 5) showed a broad maximum in the afternoon in both campaigns, which may be related to the transport of polluted air from the lowland areas due to strong daytime convective mixing within the planetary boundary layer (PBL) (Gao et al. 2005; Ren et al. 2009). The summer campaign had a more distinct diurnal

Table 2 Comparison with data from other mountainous and surface sites

Measurement site	Altitude	Period	SO_4^{2-}	NO_3^-	NH_4^+	References
Mountain site						
Mt. Tai, China	1,534 m	Mar.–Apr. 2007	12.76±8.83	5.81±4.71	5.55±3.86	This study
		Jun.–Jul. 2007	22.92±16.73	4.03±4.00	8.03±6.29	
Mt. Zeppelin,Finland	470 m	Feb.–Mar. 2001	0.849±0.509[a]	0.041±0.042	0.069±0.053	Teinila et al. 2004
		Apr.–May 2001	1.79±2.19[a]	0.053±0.037	0.083±0.031	
Great Smoky Mnts NP, USA[b]	810 m	Jul.–Aug 2004	7.74±3.95	0.16±0.21	1.69±0.91	Lee et al. 2008
Yosemite NP, USA[b]	1,603 m	Jun.–Sep. 2002	1.01±0.42	0.30±0.21	0.36±0.16	Lee et al. 2008
San Gorgonio, USA[b]	1,705 m	Apr. 2003	0.61±0.86	3.19±4.98	0.90±1.28	Lee et al. 2008
		Jul. 2003	1.33±0.69	1.29±2.41	0.95±0.99	
Mt.Tateyama, Japan[c]	2,450 m	spring 1996–2000	2.26	0.64	0.91	Kido et al. 2001
Mt. Fuji, Japan	3,770 m	Jul.–Aug. 1993	1.24	0.04	0.02	Tsuboi et al. 1996
Mt. Waliguan, China[d]	3,816 m	Oct. 1994	0.22±0.10	0.24±0.10	0.33±0.18	Yang et al. 1996
Zhuzhang, China[e]	3,583 m	Jul.2004–Mar.2005	1.6±0.77	0.45±0.34	0.15±0.14	Qu et al. 2009
Ground site						
Jinan, China (urban)	15 m	spring 2005	20.7	11.9	8.2	Yang et al. 2007
		summer 2005	29.9	3.4	13.3	
Shanghai, China (urban)	15 m	spring 2004	11.73	9.05	4.05	Wang et al. 2006
		summer 2004	5.43	2.59	2.44	
Shanghai, China (rural)	Ground	summer 2005	15.8±9.8	7.1±6.7	4.1±1.5	Pathak et al. 2009
Beijing, China (urban and rural)	40 m	spring 2001–2003	13.52±13.95	11.92±11.79	6.47±6.75	Wang et al. 2005
		summer 2001–2003	18.42±15.28	11.18±10.37	10.10±6.97	
Beijing, China (rural)	Ground	summer 2005	22.6±26.1	9.9±12.0	4.7±3.3	Pathak et al. 2009

[a] nss-SO_4^{2-}

[b] Using the PILS method

[c] Non-precipitation conditions

[d] TSP

[e] Aerosol less than 10 μm in diameter

pattern than spring. The average SOR in summer was 57% (±27%), which is more than twice that in spring (24±16%), indicating stronger oxidation of SO_2 to form sulfate in summer. It is known that SO_2 is converted to sulfate particles via gas-phase, heterogeneous, or multiphase processes (Pandis and Seinfeld 1989). The gas-phase oxidation only occurs in daytime at a relatively slow rate of ~1% per hour (Newman 1981), and is affected by temperature and solar radiation. Aqueous oxidation in a typical cloud, on the other hand, can occur at a rate of 1,000% per hour (Pandis and Seinfeld 1989). The oxidation rates in the troposphere are determined by 1) the presence of clouds and fogs, 2) the concentrations of oxidants such as H_2O_2 and O_3, and 3) sunlight intensity. The large values of SOR in summer at Mt. Tai can be explained by stronger photochemical and in-cloud processes leading to higher production of sulfate in summer. Thus the higher sulfate concentrations in summer than in spring is attributed to the much faster conversion of SO_2 to sulfate in summer despite the lower concentrations of SO_2 (see Fig. 5).

In contrast, the average NOR in spring and summer were comparable 11% (±10%) vs. 9% (±6%), with lower concentrations of fine nitrate in summer (see Table 1) due to the smaller abundance of reactive nitrogen in summer (Fig. 5). The comparable apparent conversion rates of fine nitrate in the two seasons can be explained by the following. Apart from the photochemical reactions that oxidize NO_x to HNO_3, the concentrations of fine

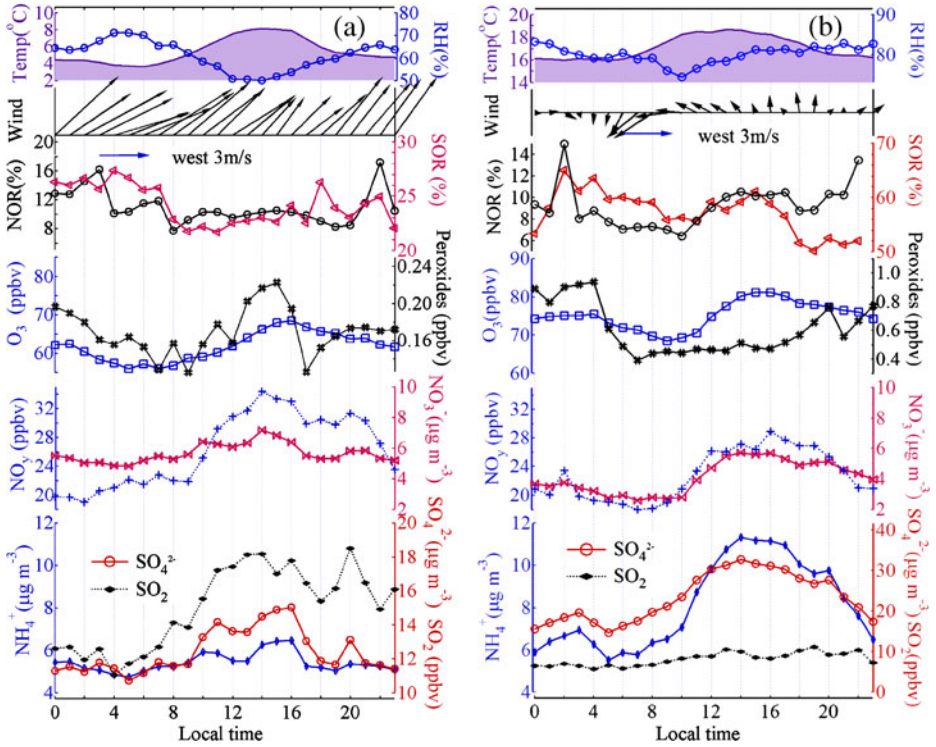

Fig. 5 Average diurnal variations of water-soluble ions, trace gases, and meteorological parameters: **a** spring campaign; **b** summer campaign

nitrate was also determined by the equilibrium between gas-phase nitric acid and particle nitrate: NH_3 (g) + HNO_3 (g) ⇋ NH_4NO_3 (s), which is temperature dependent. The higher temperature in summer promotes faster production of HNO_3 and increases emission of NH_3, but at the same time leads to larger disassociation of particulate nitrate. Additionally, twice as much sulfate in summer at Mt. Tai indicates that large amount of H_2SO_4 produced from SO_2 oxidation in summer competes with HNO_3 for NH_3 which could lead to a slower production of nitrate.

Figure 5 shows that in spring the afternoon concentration peaks (~14 $\mu g m^{-3}$) of SO_4^{2-} (and NH_4^+) corresponded to those of O_3 and peroxides, but the SOR decreased; in summer the SO_4^{2-} daytime maximum (~30 $\mu g m^{-3}$) coincided to O_3 and SOR, but to a minimum in peroxide concentration. The latter may be due to aqueous-phase S (IV) oxidation by peroxides under frequent cloudy conditions. For NOR, its variation generally followed that of relative humidity (RH), but was opposite to the variation of temperature in spring, though no obvious variation was observed in the daytime. In summer, an evident NOR peak was detected at ~15:00 LT, corresponding to a NO_y maximum. In both seasons, the mean NOR was higher at night.

The SOR (spring: 24±16%, summer: 57±27%) at Mt. Tai are comparable to the values observed at the acid rain-stressed Whiteface Mountain in the eastern US from 1988 to 1994 (March to April: 25%; June to July: 57%) (Dutkiewicz et al. 2000). The ratios at the mountain-top sites are higher than those observed at a urban site near Whiteface Mountain

(Dutkiewicz et al. 2000) and in Nagoya, Japan (Kido et al. 2001), suggesting more active cloud processing at the mountain tops. The fine nitrate oxidation ratios at Mt. Tai were found comparable to a previous study at an urban surface site (Kadowaki 1986).

3.3 Factors influencing the variations of $PM_{2.5}$ ions

To further elucidate the major factors that affected variations of $PM_{2.5}$ ions, a principal component analysis (PCA) (Buhr et al. 1996; Johnson and Wichern 1998) was applied to the data collected during the two campaigns.

3.3.1 Spring

A total of 15 variables, including nss-SO_4^{2-}, NO_3^-, NH_4^+, K^+, Ca^{2+}, Na^+, Cl^-, SO_2, NO_y, O_3, OC, EC, CO, total peroxides, and RH were selected for the PCA analysis in spring. The factor loadings and the percentage of the variance explained by each factor are shown in Table 3. Together, five factors account for 74% of the total variance. The first factor, with the maximum explained variance (35%), possessed large contributions from nss-SO_4^{2-}, NO_3^-, NH_4^+, K^+ and SO_2, which was associated with aged or processed air masses, representing long range transport. Factor 2 was principally composed of SO_2, NO_y, OC, EC and CO with a variance of 15%, and was related to fresh emissions from combustion sources. Factor 3 was mainly comprised of Ca^{2+}, Mg^{2+} and Na^+ which represent crustal or soil dust; two dust storms were observed in the spring campaign. Factor 4 was primarily made up of contributions from Na^+ and Cl^- with a variance of 8%, and was attributed to sea salt. Interestingly, a high loading of EC was also shown in the fourth factor perhaps suggesting that the sea salt particles had undergone cloud processing and became internally

Table 3 Factor loadings from principal component analysis (spring campaign)

Spring	Factor 1	Factor 2	Factor 3	Factor 4	Factor 5
nss-SO_4^{2-}	**0.88**	0.19	0.10	0.06	−0.11
NO_3^-	**0.88**	0.19	−0.11	0.06	−0.01
NH_4^+	**0.92**	0.22	−0.08	0.14	−0.04
K^+	**0.72**	0.18	0.24	0.31	0.07
Ca^{2+}	0.00	0.03	**0.93**	0.07	−0.04
Mg^{2+}	0.09	0.05	**0.92**	0.11	0.01
Na^+	0.07	−0.06	**0.42**	**0.72**	0.22
Cl^-	0.49	−0.02	−0.05	**0.65**	0.10
SO_2	**0.60**	**0.51**	0.16	0.02	0.07
NO_y	0.35	**0.75**	−0.07	−0.09	0.23
O_3	0.39	0.40	**−0.31**	0.01	−0.39
OC	0.11	**0.81**	0.09	0.17	−0.14
EC	0.09	**0.57**	−0.01	**0.65**	−0.08
CO	0.34	**0.69**	0.01	−0.05	0.38
Peroxides	0.16	−0.02	−0.07	−0.10	**−0.75**
RH	0.33	0.24	**−0.31**	0.10	**0.57**
Variance	35%	15%	10%	8%	6%

Values in bold indicate loading factors discussed in this paper

or externally mixed with EC during transport (Spencer et al. 2008). Factor 5 had a positive contribution from RH and a negative contribution from peroxides, indicative of the impact of clouds (Ren et al. 2009); this factor contributed about 6% of the total variance.

3.3.2 Summer

In the summer campaign, the Na^+ and Cl^- concentrations were below the MDL for most observations, and were excluded from PCA analysis. Four major factors were obtained accounting for 79% of the total variance (Table 4).

The first factor had positive contributions from nss-SO_4^{2-}, NO_3^-, NO_y, NH_4^+, O_3, K^+, OC, EC and NO_y with a variance of 46%. This factor can be interpreted as moderately processed air masses from the boundary layer. Factor 2 was comprised principally of a positive loading of RH and a negative loading from peroxides, indicating the influence of clouds and fog, and is similar to factor 5 in spring. This factor explained 15% of the total variance in summer. The third factor had strong positive loadings of SO_2, CO, and a moderate loading of K^+, attributed to fossil fuel and biomass burning. The contribution of biomass burning will be examined in Section 3.5. Factor 4 had strong loadings from Ca^{2+} and Mg^{2+} representing crustal and soil dust contributions; this factor contributed to 6% of the total variance in summer (compared to 10% in spring).

In summary, the PCA indicates that trace gases and aerosols at Mt. Tai during the two campaigns were principally derived from the transport of pollution (fresh, moderately-, or well-processed), cloud/fog processing, and crustal sources.

3.4 Scavenging of water soluble ions by clouds/fogs

An examination of diurnal variations and the results of the PCA indicated rapid decreases in the concentrations of measured ions during cloud or fog events at Mt. Tai. In the spring and

Table 4 Factor loadings from principal component analysis (summer campaign)

Summer	Factor 1	Factor 2	Factor 3	Factor 4
nss-SO_4^{2-}	**0.82**	0.07	0.40	−0.03
NO_3^-	**0.85**	0.17	0.17	0.09
NH_4^+	**0.84**	0.18	0.27	0.00
K^+	**0.58**	−0.08	**0.54**	0.40
Ca^{2+}	−0.01	0.07	0.00	**0.94**
Mg^{2+}	0.13	−0.06	0.14	**0.91**
SO_2	0.30	−0.01	**0.84**	0.15
NO_y	**0.75**	0.23	0.40	0.09
O_3	**0.67**	−0.30	0.40	0.07
OC	**0.80**	0.08	0.18	0.07
EC	**0.74**	0.31	−0.12	0.07
CO	0.32	**0.53**	**0.62**	−0.11
Peroxides	−0.23	**−0.85**	−0.10	−0.06
RH	0.07	**0.93**	−0.05	−0.03
Variance	46%	15%	12%	6%

Values in bold indicate loading factors discussed in this paper

summer campaigns, 15% and 39% of days, respectively, were under cloudy or rainy conditions. The continuous data from the AIM allowed us to examine the scavenging of ions by clouds at Mt. Tai. The diurnal variation of $PM_{2.5}$ water-soluble ions, trace gases, and meteorological parameters on a cloudy day in spring (April 17) and another in summer (June 19) is presented in Fig. 6. There were five additional cloud events (two in the spring and three in the summer, figure not shown).

Aerosol ionic concentrations had a high concentration and a broad afternoon peak before the onset of clouds, and decreased sharply after the occurrence of cloud in late afternoon or evening.

Assuming that the concentration decrease follows $dC/dt = -rC$, we can obtain $C_{(t)} = C_0 e^{-rt}$, where C_0, stands for the initial concentration. The constant r (unit=h^{-1}) may be considered as a scavenging rate constant, with a larger value representing a larger extent of scavenging. Exponential fits to the concentration data of SO_4^{2-}, NO_3^-, and NH_4^+ on June 19 are presented in Fig. 7, giving a scavenging rate constant of 0.33, 0.64 and 0.50 h^{-1}, for sulfate, nitrate, and ammonium, respectively. The rate constants for $PM_{2.5}$, other ions, OC, and EC on June 19 and for additional six events are listed in Table 5.

To see whether the drops in aerosol concentrations were related to a change in air mass during the cloud events, we examined the concurrently measured CO, which is not water soluble, and thus whose concentrations should not be affected by clouds. Although CO may not be emitted by the same source(s) as $PM_{2.5}$ and ions, all have higher concentrations in the polluted parts of the Planetary Boundary Layer, and are thus expected to have good correlations (r=0.66 for data collected on clear days). The rates of CO concentration

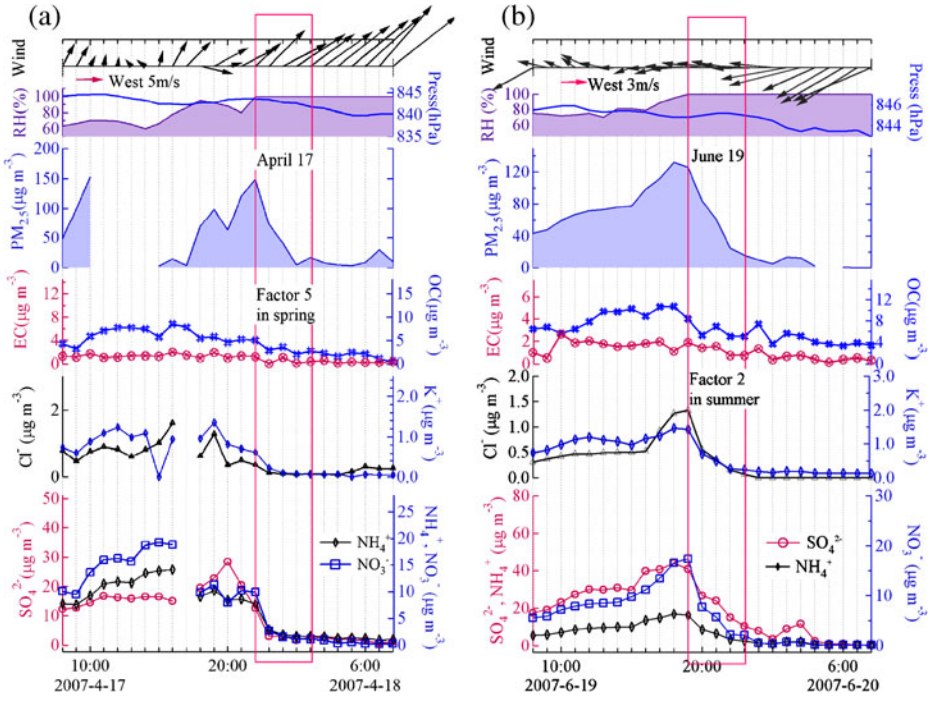

Fig. 6 Major ion concentrations and meteorological parameters during two cloud events: **a** April 17, 2007; **b** June 19, 2007

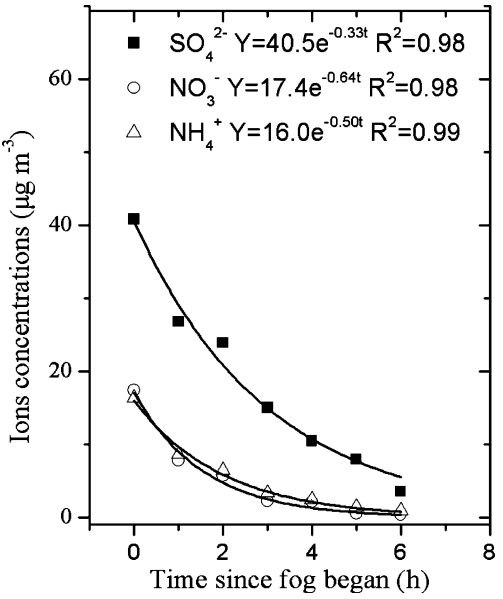

Fig. 7 Scavenging rates of major compounds in $PM_{2.5}$ during the cloud event on June 19, 2007

changes during cloud events were much smaller than those of decrease in aerosol concentrations (with the former being 1–30% of the aerosol decrease rates). This suggests that the decreases in $PM_{2.5}$ and ionic concentrations during clouds were predominantly due to cloud scavenging, not changes in chemical loading of air masses.

Table 5 shows that the scavenging rate constants varied for different ions in a cloud event and for the same ion in different cloud events. Previous studies have shown that scavenging of ions by clouds may depend on liquid water content (LWC) of the cloud, PM concentration, and the mixing state of the aerosols (Hallberg et al. 1992; Hitzenberger et al. 2001; Sellegri et al. 2003). In Table 5, slower rates of cloud scavenging on June 19, July 9 and July 12 are associated with a low LWC, compared to larger rates on March 30 and April 18 with higher LWC.

Figure 8 illustrates the scavenging rates as a function of average $PM_{2.5}$ during the events that captured LWC information (March 30, April 18, June 19 and 26). In general, larger scavenging rates of ion and EC were observed at low $PM_{2.5}$ concentrations. This is consistent with other studies indicating a negative correlation between the scavenging efficiencies for sulfate and black carbon (BC) and total aerosol concentration (Hallberg et al. 1992; Hallberg et al. 1994; Gieray et al. 1997). Ammonium had smaller scavenging rates compared to sulfate and nitrate in most cases, but the reason for this phenomenon is unclear. Larger scavenging rates were observed for EC than OC in most of the events, perhaps suggesting internal mixing of EC with more hygroscopic species, such as sulfate and nitrate and external mixing between inorganic and organic aerosols (Sellegri et al. 2003).

3.5 Biomass burning in summer

Previous studies have shown that the burning of crop residues is an important source of trace gases and aerosols in the central-eastern plains during the summer (Wang et al. 2002; Ding et al. 2008). A recent analysis of hydrocarbons obtained at the top of Mt. Tai also

Table 5 Summary of scavenging rate constants of $PM_{2.5}$ mass and major compounds

Events	Scavenging rate constant (h^{-1})										Average LWC ($\times 10^{-4}$ Lm^{-3})	Average $PM_{2.5}$ (μgm^{-3})
	Cloud start (LT)	Cloud duration (h)	$PM_{2.5}$	SO_4^{2-}	NO_3^-	NH_4^+	K^+	Cl^-	EC	OC		
20070330	16:00	3	0.92	1.21	1.02	0.69	0.74	0.59	[a]	[a]	0.70	34.8
20070417	22:00	4	0.74	1.04	1.12	0.74	0.96	0.79	[a]	0.25	[a]	52.0
20070418	17:00	3	1.09	1.39	1.18	0.75	0.92	1.29	1.31	0.72	1.50	15.7
20070619	19:00	7	0.47	0.33	0.64	0.50	0.51	0.76	0.18	0.12	0.30	46.7
20070626	16:00	7	0.50	0.53	0.55	0.40	0.40	0.46	0.27	0.08	1.30	46.8
20070709	22:00	3	0.37	0.41	0.23	0.30	0.21	0.32	0.60	[b]	[b]	39.1
20070712	19:00	6	0.52	0.42	0.37	0.31	0.38	0.49	0.28	0.12	[b]	66.6

[a] No data

[b] Below MDL

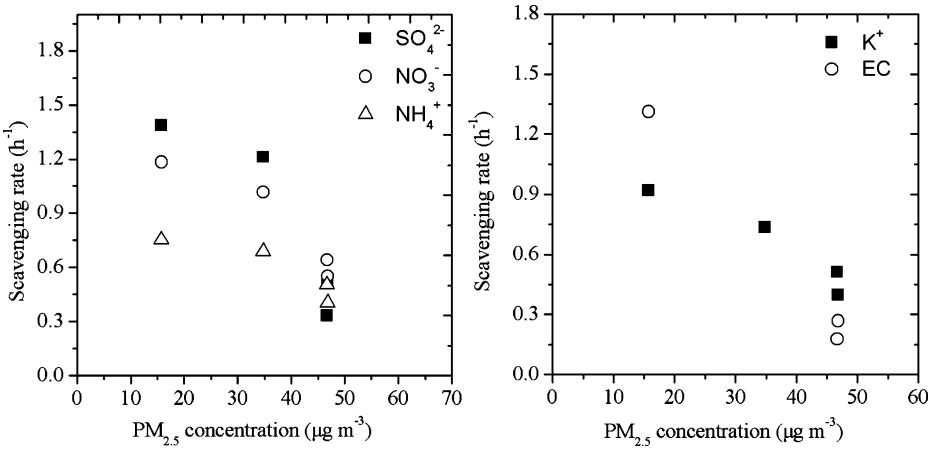

Fig. 8 Scavenging rates for major ion concentrations and EC as a function of average $PM_{2.5}$ concentrations during the cloud events on March 30, April 18, June 19 and 26, 2007

indicated the impact of crop burning in the summer of 2006 (Suthawaree et al. 2010). By examining satellite images and K^+/SO_4^{2-} ratios, assuming K^+ in $PM_{2.5}$ is a marker for biomass burning (Andreae 1983; Ma et al. 2003), we found evidence for more intensive burning during the first half of the summer campaign (June 15–30) compared with the second half (July 1–15). The mean molar K^+/SO_4^{2-} ratio in the first period was 0.13±0.09 compared with 0.08±0.06 in July ($p<0.01$). In addition, more numerous fire counts (http://maps.geog.umd.edu/firms/) were observed in the MODIS sensor aboard the Aqua & Terra satellite during June 15–30 (Fig. 9). Additionally, larger molar ratios of oxalate to sulfate were found in June compared to July (the filter data was 0.017 versus 0.007, respectively); previous studies have suggested that biomass burning is an important source of oxalate (Narukawa et al. 1999; Yamasoe et al. 2000).

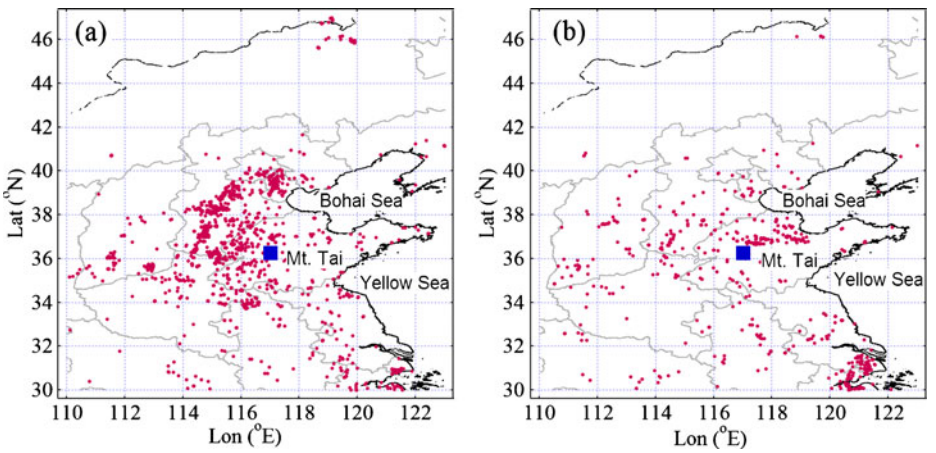

Fig. 9 Fire counts over central-eastern China from Aqua & Terra-MODIS: **a** June 15–30, 2007; **b** July1–15, 2007

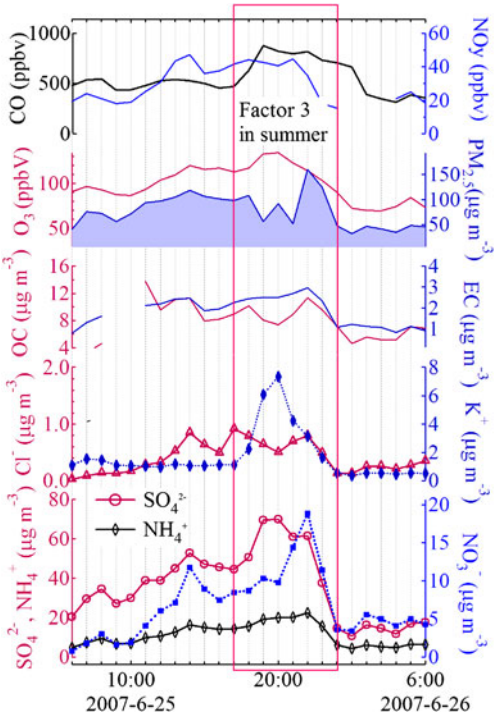

Fig. 10 Variation in major water soluble ions, trace gases, other aerosol components, and meteorological parameters observed at Mt. Tai during a biomass-burning event (June 25, 2007)

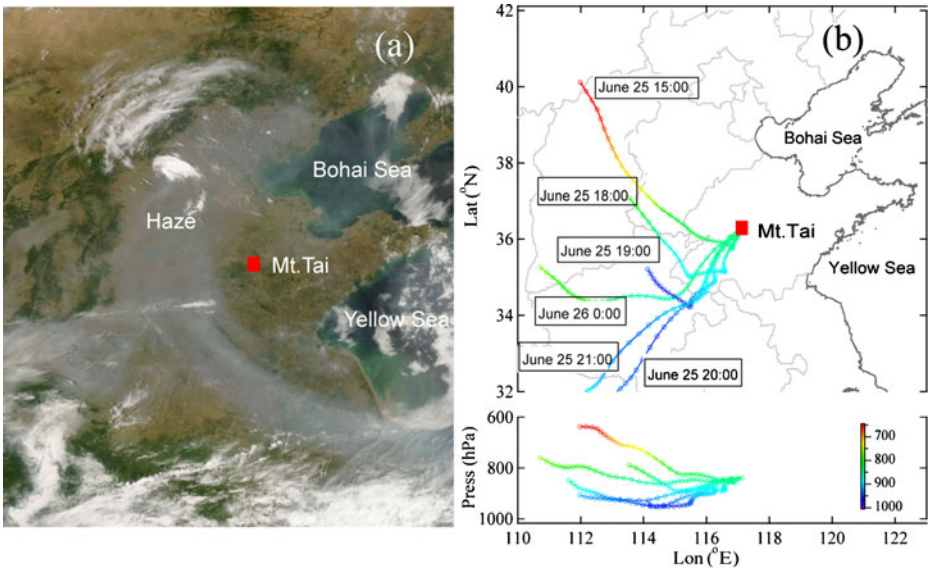

Fig. 11 MODIS true color image taken on June 25, 2007 **a** and 36-hour backward trajectories of air mass arriving at the summit of Mt. Tai **b**

The most obvious impact of biomass burning at the summit of Mt. Tai was observed on June 25 when the highest concentration of K^+ (7.4 $\mu g m^{-3}$) was observed for the whole summer campaign. Figure 10 shows the variation of water-soluble ions (including K^+), trace gases, and meteorological parameters over 24 h on June 25–26. The concentrations of O_3, CO, SO_4^{2-} and K^+ reached their maximum at about 20:00. On this day, the observed amount of O_3 and sulfate also reached their highest concentrations (134 ppbv and 70.0 $\mu g m^{-3}$, respectively) in the whole summer campaign. A MODIS true color image shows that an arc-shaped haze formed over eastern China on June 25 (Fig. 11; http://earthobservatory.nasa.gov). Thirty-six hour backward trajectories were calculated using the online version of the Hybrid Single-Particle Lagrangian Integrated Trajectory (HYSPLIT) model (accessed via http://www.arl.noaa.gov/ready/open/hysplit4.html) to learn about the origin and transport pathway of the air parcels arriving at the site. The results show that air masses arriving at 20:00 (LT) passed over the burning areas from the lower part of PBL, in agreement with the in-situ chemical data indicating transport of surface pollution to the summit. The chemical data showed that prior to the peak caused by the burned biomass plume; air mass characteristic of fossil fuel burning had arrived at the site. Namely, the concentrations of NO_y, SO_2, EC, OC, and $PM_{2.5}$ had increased in the late morning while the level of K^+ was lower (Fig. 10). The high correlation of K^+ with SO_4^{2-} (R^2=0.92) during the late evening indicates K^+ may exist as K_2SO_4 which is often present in aged smoke through reactions between biomass burning and other sources (Li et al. 2003). This suggests that the polluted air masses on this day were mixed fossil fuel and biomass burning emissions with an increasing contribution from the latter in the evening.

4 Summary and conclusion

$PM_{2.5}$ ionic compositions were made near real-time, in conjunction with a suite of other trace gas and aerosol measurements, in the spring and summer of 2007 at the summit of Mt. Tai. The results confirmed that Mt. Tai suffers more serious pollution compared to other rural mountain sites. Transport of pollution sources from the lower PBL was evident from enhanced daytime concentrations of SO_4^{2-}, NO_3^-, and NH_4^+. Sulfate contributed 57% of the molar concentration of total oxidized sulfur in summer, compared to 24% in spring, indicating strong photochemical and cloud processing in the summertime. Polluted air masses (fresh, moderately-aged and well-aged) were observed at the sampling site; the impact of dust storms and biomass burning was observed in spring and summer, respectively. Cloud scavenging rates showed large variations for different ions and in different cloud events. The high concentrations of water soluble ions and the strong formation of sulfate at this high-elevation site reveal that serious aerosol pollution in central-eastern China exists not only at the surface, but also at the top of the planetary boundary layer. The data from this study will be useful for assessing the formation of acid rain and the impact of aerosols on radiative forcing in eastern China.

Acknowledgments The authors would like to acknowledge Steven Poon, Wang Jin, Zhou Xuehua, Sun Tingli, Nie Wei, and Xu Pengju for their help in organizing the field study and in setting up the instruments. We thank Ding Aijun for providing Figure 1; Ren Yu, Zhang Jiamin, Jeffrey Collett and Guo Jia for their contributions to the measurements of peroxide, reactive nitrogen and LWC of the clouds; and Shou Youping and Wang Jing for their assistance in laboratory analysis. We are also grateful to the Mt. Tai Meteorological Observatory for its support of the field study and for providing meteorological data. The HYSPLIT model was provided by the NOAA Air Resources Laboratory. Fire detection data was provided by http://maps.geog.

umd.edu/firms/. This research was funded by the National Basic Research Program of China (973 Project No. 2005CB422203), Shandong Provincial Environmental Protection Department (2006045), and the Hong Kong Polytechnic University's Niche Area Development Scheme (1-BB94).

References

Anderson, R.R., Martello, D.V., Rohar, P.C., Strazisar, B.R., Tamilia, J.P., Waldner, K., White, C.M., Modey, W.K., Mangelson, N.F., Eatough, D.J.: Sources and composition of $PM_{2.5}$ at the National Energy Technology Laboratory in Pittsburgh during July and August 2000. Energy Fuels **16**, 261–269 (2002)

Andreae, M.: Soot carbon and excess fine potassium: long-range transport of combustion-derived aerosols. Science **220**, 1148 (1983)

Andreae, M.O., Rosenfeld, D.: Aerosol-cloud-precipitation interactions. Part 1. The nature and sources of cloud-active aerosols. Earth Sci. Rev. **89**, 13–41 (2008)

Buhr, M., Sueper, D., Trainer, M., Goldan, P., Kuster, B., Fehsenfeld, F., Kok, G., Shillawski, R., Schanot, A.: Trace gas and aerosol measurements using aircraft data from the North Atlantic Regional Experiment (NARE 1993). J. Geophys. Res. **101**, 29013–29027 (1996)

Ding, A.J., Wang, T., Thouret, V., Cammas, J.P., Nedelec, P.: Tropospheric ozone climatology over Beijing: analysis of aircraft data from the MOZAIC program. Atmos. Chem. Phys. **8**, 1–13 (2008)

Dutkiewicz, V.A., Das, M., Husain, L.: The relationship between regional SO_2 emissions and downwind aerosol sulfate concentrations in the Northeastern US. Atmos. Environ. **34**, 1821–1832 (2000)

Gao, J., Wang, T., Ding, A.J., Liu, C.: Observational study of ozone and carbon monoxide at the summit of mount Tai (1534 m a.s.l.) in central-eastern China. Atmos. Environ. **39**, 4779–4791 (2005)

Gieray, R., Wieser, P., Engelhardt, T., Swietlicki, E., Hansson, H., Mentes, B., Orsini, D., Martinsson, B., Svenningsson, B.: Phase partitioning of aerosol constituents in cloud based on single-particle and bulk analysis. Atmos. Environ. **31**, 2491–2502 (1997)

Grover, B.D., Eatough, N.L., Eatough, D.J., Chow, J.C., Watson, J.G., Ambs, J.L., Meyer, M.B., Hopke, P. K., Al-Horr, R., Later, D.W., Wilson, W.E.: Measurement of both nonvolatile and semi-volatile fractions of fine particulate matter in Fresno CA. Aerosol Sci. Technol. **40**, 811–826 (2006)

Hallberg, A., Ogren, J., Noone, K., Heintzenberg, J., Berner, A., Solly, I., Kruisz, C., Reischl, G., Fuzzi, S., Facchini, M.: Phase partitioning for different aerosol species in fog. Tellus Ser. B **44**, 545–555 (1992)

Hallberg, A., Ogren, J., Noone, K., Okada, K., Heintzenberg, J., Svenningsson, I.: The influence of aerosol particle composition on cloud droplet formation. J. Atmos. Chem. **19**, 153–171 (1994)

Hirsch, R., Gilroy, E.: Methods of fitting a straight line to data: examples in water resources. J. Am. Water Resour. Assoc. **20**, 705–711 (1984)

Hitzenberger, R., Berner, A., Glebl, H., Drobesch, K., Kasper-Giebl, A., Loeflund, M., Urban, H., Puxbaum, H.: Black carbon (BC) in alpine aerosols and cloud water—concentrations and scavenging efficiencies. Atmos. Environ. **35**, 5135–5141 (2001)

Johnson, R., Wichern, D.: Applied multivariate statistical analysis. Prentice Hall Englewood Cliffs, NJ (1998)

Kadowaki, S.: On the nature of atmospheric oxidation processes of sulfur dioxide to sulfate and of nitrogen dioxide to nitrate on the basis of diurnal variations of sulfate, nitrate, and other pollutants in an urban area. Environ. Sci. Technol. **20**, 1249–1253 (1986)

Kido, M., Osada, K., Matsunaga, K., Iwasaka, Y.: Diurnal variation of ionic aerosol species and water-soluble gas concentrations at a high-elevation site in the Japanese Alps. J. Geophys. Res. **106**, 17335–17345 (2001)

Lazrus, A.L., Kok, G.L., Lind, J.A., Gitlin, S.N., Heikes, B.G., Shetter, R.E.: Automated fluorometric method for hydrogen peroxide in air. Anal. Chem. **58**, 594–597 (1986)

Lee, T., Yu, X.-Y., Kreidenweis, S.M., Malm, W.C., Collett, J.L.: Semi-continuous measurement of $PM_{2.5}$ ionic composition at several rural locations in the United States. Atmos. Environ. **42**, 6655–6669 (2008)

Li, J., Posfai, M., Hobbs, P.V., Buseck, P.R.: Individual aerosol particles from biomass burning in southern Africa: 2. Compositions and aging of inorganic particles. J. Geophys. Res. (2003). doi:10.1029/2002jd002310

Li, J., Wang, Z.F., Akimoto, H., Gao, C., Pochanart, P., Wang, X.Q.: Modeling study of ozone seasonal cycle in lower troposphere over east Asia. J. Geophys. Res. (2007). doi:10.1029/2006jd008209

Ma, Y., Weber, R.J., Lee, Y.N., Orsini, D.A., Maxwell-Meier, K., Thornton, D.C., Bandy, A.R., Clarke, A.D., Blake, D.R., Sachse, G.W., Fuelberg, H.E., Kiley, C.M., Woo, J.H., Streets, D.G., Carmichael, G.R.: Characteristics and influence of biosmoke on the fine-particle ionic composition measured in Asian outflow during the Transport and Chemical Evolution Over the Pacific (TRACE-P) experiment. J. Geophys. Res. (2003). doi:10.1029/2002jd003128

Narukawa, M., Kawamura, K., Takeuchi, N., Nakajima, T.: Distribution of dicarboxylic acids and carbon isotopic compositions in aerosols from 1997 Indonesian forest fires. Geophys. Res. Lett. **26**, 3101–3104 (1999)

Nel, A.: Air pollution-related illness: effects of particles. Science **308**, 804–806 (2005)

Newman, L.: Atmospheric oxidation of sulfur dioxide: a review as viewed from power plant and smelter plume studies. Atmos. Environ. **15**, 2231–2239 (1981)

Nie, W., Wang, T., Gao, X., Pathak, R.K., Wang, X., Gao, R., Zhang, Q., Yang, L., Wang, W.: Comparison among filter-based, impactor-based and continuous techniques for measuring atmospheric fine sulfate and nitrate. Atmos. Environ. **44**, 4396–4403 (2010)

Ocskay, R., Salma, I., Wang, W., Maenhaut, W.: Characterization and diurnal variation of size-resolved inorganic water-soluble ions at a rural background site. J. Environ. Monit. **8**, 300–306 (2006)

Orsini, D.A., Ma, Y.L., Sullivan, A., Sierau, B., Baumann, K., Weber, R.J.: Refinements to the particle-into-liquid sampler (PILS) for ground and airborne measurements of water soluble aerosol composition. Atmos. Environ. **37**, 1243–1259 (2003)

Pandis, S., Seinfeld, J.: Sensitivity analysis of a chemical mechanism for aqueous-phase atmospheric chemistry. J. Geophys. Res. **94**, 1105–1126 (1989)

Pathak, R.K., Chan, C.K.: Inter-particle and gas-particle interactions in sampling artifacts of $PM_{2.5}$ in filter-based samplers. Atmos. Environ. **39**, 1597–1607 (2005)

Pathak, R.K., Wu, W.S., Wang, T.: Summertime $PM_{2.5}$ ionic species in four major cities of China: nitrate formation in an ammonia-deficient atmosphere. Atmos. Chem. Phys. **9**, 1711–1722 (2009)

Qu, W.J., Zhang, X.Y., Arimoto, R., Wang, Y.Q., Wang, D., Sheng, L.F., Fu, G.: Aerosol background at two remote CAWNET sites in western China. Sci. Total Environ. **407**, 3518–3529 (2009)

Ren, Y., Ding, A.J., Wang, T., Shen, X.H., Guo, J., Zhang, J.M., Wang, Y., Xu, P.J., Wang, X.F., Gao, J., Collett, J.L.: Measurement of gas-phase total peroxides at the summit of Mount Tai in China. Atmos. Environ. **43**, 1702–1711 (2009)

Saarnio, K., Aurela, M., Timonen, H., Saarikoski, S., Teinila, K., Makela, T., Sofiev, M., Koskinen, J., Aalto, P.P., Kulmala, M., Kukkonen, J., Hillamo, R.: Chemical composition of fine particles in fresh smoke plumes from boreal wild-land fires in Europe. Sci. Total Environ. **408**, 2527–2542 (2010)

Sellegri, K., Laj, P., Dupuy, R., Legrand, M., Preunkert, S., Putaud, J.P.: Size-dependent scavenging efficiencies of multicomponent atmospheric aerosols in clouds. J. Geophys. Res. (2003). doi:10.1029/2002jd002749

Solomon, P.A., Sioutas, C.: Continuous and semicontinuous monitoring techniques for particulate matter mass and chemical components: a synthesis of findings from EPA's particulate matter supersites program and related studies. J. Air Waste Manage. Assoc. **58**, 164–195 (2008)

Spencer, M.T., Holecek, J.C., Corrigan, C.E., Ramanathan, V., Prather, K.A.: Size-resolved chemical composition of aerosol particles during a monsoonal transition period over the Indian Ocean. J. Geophys. Res. (2008). doi:10.1029/2007JD008657

Streets, D.G., Bond, T.C., Carmichael, G.R., Fernandes, S.D., Fu, Q., He, D., Klimont, Z., Nelson, S.M., Tsai, N.Y., Wang, M.Q., Woo, J.H., Yarber, K.F.: An inventory of gaseous and primary aerosol emissions in Asia in the year 2000. J. Geophys. Res. (2003). doi:10.1029/2002jd003093

Suthawaree, J., Kato, S., Okuzawa, K., Kanaya, Y., Pochanart, P., Akimoto, H., Wang, Z., Kajii, Y.: Measurements of volatile organic compounds in the middle of Central East China during Mount Tai Experiment 2006 (MTX2006): observation of regional background and impact of biomass burning. Atmos. Chem. Phys. **10**, 1269–1285 (2010)

Teinila, K., Hillamo, R., Kerminen, V.M., Beine, H.J.: Chemistry and modal parameters of major ionic aerosol components during the NICE campaigns at two altitudes. Atmos. Environ. **38**, 1481–1490 (2004)

Trebs, I., Meixner, F.X., Slanina, J., Otjes, R., Jongejan, P., Andreae, M.O.: Real-time measurements of ammonia, acidic trace gases and water-soluble inorganic aerosol species at a rural site in the Amazon Basin. Atmos. Chem. Phys. **4**, 967–987 (2004)

Tsai, C.J., Perng, S.N.: Artifacts of ionic species for hi-vol PM_{10} and PM_{10} dichotomous samplers. Atmos. Environ. **32**, 1605–1613 (1998)

Tsuboi, K., Hosomi, T., Dokiya, Y., Tsutsumi, Y., Yanagisawa, K., Tanaka, S.: Chemical species in aerosol, gases and precipitation at summit of Mt. Fuji. J. Aerosol Res. (in Japanese) **11**, 226–234 (1996)

Vecchi, R., Chiari, M., D'Alessandro, A., Fermo, P., Lucarelli, F., Mazzei, F., Nava, S., Piazzalunga, A., Prati, P., Silvani, F., Valli, G.: A mass closure and PMF source apportionment study on the sub-micron sized aerosol fraction at urban sites in Italy. Atmos. Environ. **42**, 2240–2253 (2008)

Wang, T., Cheung, T.F., Li, Y.S., Yu, X.M., Blake, D.R.: Emission characteristics of CO, NOx, SO_2 and indications of biomass burning observed at a rural site in eastern China. J. Geophys. Res. (2002). doi:10.1029/2001jd000724

Wang, T., Poon, C.N., Kwok, Y.H., Li, Y.S.: Characterizing the temporal variability and emission patterns of pollution plumes in the Pearl River Delta of China. Atmos. Environ. **37**, 3539–3550 (2003a)

Wang, T., Ding, A.J., Blake, D.R., Zahorowski, W., Poon, C.N., Li, Y.S.: Chemical characterization of the boundary layer outflow of air pollution to Hong Kong during February–April 2001. J. Geophys. Res. (2003b). doi:10.1029/2002JD003272

Wang, Y., Zhuang, G.S., Tang, A.H., Yuan, H., Sun, Y.L., Chen, S.A., Zheng, A.H.: The ion chemistry and the source of $PM_{2.5}$ aerosol in Beijing. Atmos. Environ. **39**, 3771–3784 (2005)

Wang, Y., Zhuang, G., Zhang, X., Huang, K., Xu, C., Tang, A., Chen, J., An, Z.: The ion chemistry, seasonal cycle, and sources of $PM_{2.5}$ and TSP aerosol in Shanghai. Atmos. Environ. **40**, 2935–2952 (2006)

Wang, Y., Wai, K.M., Gao, J., Liu, X., Wang, T., Wang, W.: The impacts of anthropogenic emissions on the precipitation chemistry at an elevated site in North-eastern China. Atmos. Environ. **42**, 2959–2970 (2008)

Watson, J.G.: Visibility: science and regulation. J. Air Waste Manage. Assoc. **52**, 628–713 (2002)

Weber, R.J., Orsini, D., Daun, Y., Lee, Y.N., Klotz, P.J., Brechtel, F.: A particle-into-liquid collector for rapid measurement of aerosol bulk chemical composition. Aerosol Sci. Technol. **35**, 718–727 (2001)

Wilson, W.E., Grover, B.D., Long, R.W., Eatough, N.L., Eatough, D.J.: The measurement of fine particulate semivolatile material in urban aerosols. J. Air Waste Manage. Assoc. **56**, 384–397 (2006)

Wu, W.S., Wang, T.: On the performance of a semi-continuous $PM_{2.5}$ sulphate and nitrate instrument under high loadings of particulate and sulphur dioxide. Atmos. Environ. **41**, 5442–5451 (2007)

Xu, H., Wang, Y., Yang, Y., Zhao, Y., Wen, T., Wu, F.: Concentrations and size distributions of water soluble ions of atmospheric aerosol at the summit of mount Tai. Environ. Sci. (in Chinese) **29**, 305 (2008)

Yamasoe, M.A., Artaxo, P., Miguel, A.H., Allen, A.G.: Chemical composition of aerosol particles from direct emissions of vegetation fires in the Amazon Basin: water-soluble species and trace elements. Atmos. Environ. **34**, 1641–1653 (2000)

Yang, D., Yu, X., Fang, X., Wu, F., Li, X.: A study of aerosol at regional background stations and baseline station. Q. J. Appl. Meteorol. (in Chinese) **7**, 396–405 (1996)

Yang, L.X., Wang, D.C., Cheng, S.H., Wang, Z., Zhou, Y., Zhou, X.H., Wang, W.X.: Influence of meteorological conditions and particulate matter on visual range impairment in Jinan China. Sci. Total Environ. **383**, 164–173 (2007)

Zhang, Q., Jimenez, J.L., Canagaratna, M.R., Allan, J.D., Coe, H., Ulbrich, I., Alfarra, M.R., Takami, A., Middlebrook, A.M., Sun, Y.L., Dzepina, K., Dunlea, E., Docherty, K., DeCarlo, P.F., Salcedo, D., Onasch, T., Jayne, J.T., Miyoshi, T., Shimono, A., Hatakeyama, S., Takegawa, N., Kondo, Y., Schneider, J., Drewnick, F., Borrmann, S., Weimer, S., Demerjian, K., Williams, P., Bower, K., Bahreini, R., Cottrell, L., Griffin, R.J., Rautiainen, J., Sun, J.Y., Zhang, Y.M., Worsnop, D.R.: Ubiquity and dominance of oxygenated species in organic aerosols in anthropogenically-influenced Northern Hemisphere midlatitudes. Geophys. Res. Lett. (2007). doi:10.1029/2007gl029979

Zhang, Q., Streets, D.G., Carmichael, G.R., He, K.B., Huo, H., Kannari, A., Klimont, Z., Park, I.S., Reddy, S., Fu, J.S., Chen, D., Duan, L., Lei, Y., Wang, I.T., Yao, Z.L.: Asian emissions in 2006 for the NASA INTEX-B mission. Atmos. Chem. Phys. **9**, 5131–5153 (2009)